Inorganic Chemistry

Article

pubs.acs.org/IC

Uncorrelated Dynamical Processes in Tetranuclear Carboxylate Clusters Studied by Variable-Temperature ^{1}H NMR Spectroscopy.

Femke F. B. J. Janssen, Laurens C. J. M. Peters, Paul P. J. Schlebos, Jan M. M. Smits, René de Gelder, and Alan E. Rowan*

Institute for Molecules and Materials, Radboud University Nijmegen, Heyendaalseweg 135, 6525 AJ, Nijmegen, The Netherlands

Supporting Information

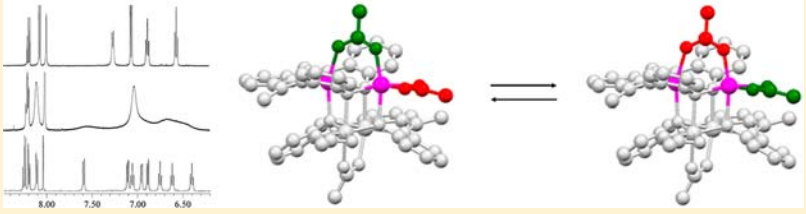

ABSTRACT: Tetranuclear carboxylate clusters with the general structural formula $[M_4(L)_2(O_2CR)_4]$ (M = Cd, Zn; LH_2 = 2,6-bis(1-(2-hydroxyphenyl)-iminoethyl)pyridine; R = CH_3, C_6H_5) were studied by variable-temperature (VT) ^{1}H NMR spectroscopy. The dynamics of these clusters in solution can be described by two uncorrelated dynamical processes. The first dynamical process is the interconversion, both inter- as well as intramolecular, between *syn*−*syn* bridging and chelating carboxylate ligands. It is shown that this carboxylate interconversion mechanism is predominantly intramolecular for $[Cd_4(L)_2(O_2CCH_3)_4]$ (**1a**), whereas for $[Zn_4(L)_2(O_2CCH_3)_4]$ (**2a**) it is predominantly intermolecular. Two models for the second dynamic process, which involves the diiminepyridine ligand, are described. The first model comprises a nondissociative rotation around an internal axis, which changes the chirality of the cluster. The second model is based on the dissociation of the tetranuclear cluster into two dimeric species, which recombine again. This last model is supported by scrambling experiments between $[Zn_4(L)_2(O_2CCH_3)_4]$ (**2a**) and $[Zn_4(L3)_2(O_2CCH_3)_4]$ (**5**) ($L3H_2$ = 2,6-bis(1-(2-hydroxyphenyl)-iminoethyl)4-chloropyridine).

INTRODUCTION

Tetranuclear (or more general polynuclear) carboxylate clusters are of interest because of their resemblance to biological systems [e.g., the oxygen evolving center (OEC) in photosystem II (PSII)][1] and their magnetic properties with potential use in, e.g., data storage, spintronics, and quantum computing.[2] The versatility in many biological systems is ascribed to the variety and flexibility of the different coordination modes of the carboxylate ligand.[3] This flexibility is reflected in the 1,2-carboxylate shift,[4] which is the interconversion of a monodentate bridging mode to a *syn*−*syn* bidentate bridging coordination mode via several possible intermediates.[3a] The switching between these coordination modes is a low-energy process that is assumed to play an important role in catalytic cycles of metalloenzymes,[5] for instance in the reaction of di-iron centers of nonheme iron enzymes with molecular oxygen.[6]

The exact nature of the role of the 1,2-carboxylate shift in the catalytic mechanism of metalloenzymes is, however, still unclear, exemplified by the studies on, e.g., the zinc metalloenzyme fanesyltransferease.[7] From several X-ray crystallographic[8] and EXAFS[9] studies two possible models are suggested for the coordination sphere around the zinc active site of this metalloenzyme, but the mechanism of catalysis is still under investigation.[7a,10] In addition to theoretical models used to understand the catalytic mechanism in metalloenzymes, synthetic mimics are studied to gain more insight into these mechanisms and the role of the carboxylate ligand.[11]

The cubic core structure of our tetranuclear clusters (Figure 1b) resembles the water-oxidizing complex in PS II.[12] This geometry of M_4O_4 clusters has been observed for a variety of metals, such as Cu,[13] Zn,[14] Ni,[15] Mn,[16] Fe,[17] and Co.[18]

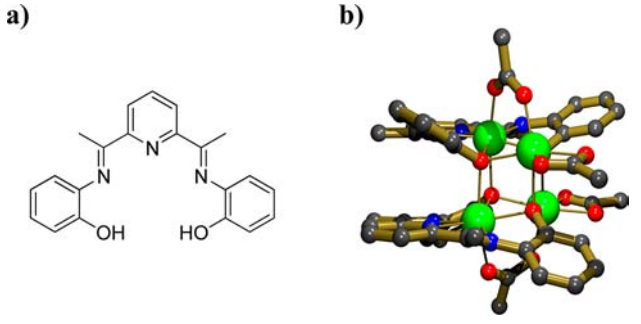

Figure 1. (a) Molecular structure of the diiminepyridine type ligand LH_2. (b) Crystal structure of the tetranuclear cluster $[M_4(L)_2(O_2CCH_3)_4]$: Zn or Cd, green; O, red; N, blue; C, gray; coordination or covalent bond, bronze.

Received: June 20, 2013
Published: October 31, 2013

   dx.doi.org/10.1021/ic401522v | *Inorg. Chem.* 2013, 52, 13004−13013

Previous research on PS II mimics has shown complicated magnetic behavior with both antiferromagnetic and ferromagnetic exchange interactions within the cluster.[19] The elucidation of the magnetic properties of $[Mn_4(L)_2(O_2CCH_3)_4]$ and its analogues with different carboxylate ligands has shown that both antiferromagnetic and ferromagnetic exchange interactions can be present depending on the type of carboxylate ligand.[20]

The tetranuclear carboxylate clusters contain two different coordination modes of the carboxylate ligand (chelating and *syn*–*syn* bridging). Studying the dynamical character of this tetranuclear compound could lead to the understanding of the functioning of metalloenzymes in catalysis and their material properties.

In this Article we report variable-temperature (VT) ^{1}H NMR spectra of tetranuclear zinc and cadmium clusters and show that the dynamics in solution can be described by two uncorrelated processes. Zinc is a common metal found in metalloenzymes,[21] and a detailed understanding of their behavior in solution through synthetic analogues is desirable. Although cadmium is regarded as being a toxic metal to most forms of life, the carbonic anhydrase (CA) in marine diatoms uses cadmium in the active center.[22] It is furthermore shown that CA is a cambialistic enzyme, meaning that it is catalytically active with zinc as well as cadmium, and that these metals can exchange easily for one another depending on the availability in the environment.[23] In our studies we compare zinc and cadmium clusters to test the effect of changing the metal center in these clusters on the dynamics. Furthermore, we discuss the influence on the rate of dynamics upon changing the carboxylate ligands from acetate to benzoate.

RESULTS AND DISCUSSION

Synthesis and Crystal Structures of $[M_4(L)_2(O_2CCH_3)_4]$ [M = Zn (1a), Cd (2a)]. The one-pot template reaction between 2,6-diacetylpyridine, 2-aminophenol, and $Zn(O_2CCH_3)_2{\cdot}2H_2O$ in methanol (Scheme 1) leads to the precipitation of an orange powder, which after recrystallization from methanol/diethylether was identified as the tetranuclear cluster $[Zn_4(L)_2(O_2CCH_3)_4]$ (**1a**) (the molecular structure of LH_2 is given in Figure 1a). A similar metal template reaction in DMF with $Cd(O_2CCH_3)_2{\cdot}2H_2O$ yielded after recrystallization from DMF/diethylether single crystals, which were identified as the tetranuclear cluster $[Cd_4(L)_2(O_2CCH_3)_4]$ (**2a**) (Table 1).[24] Both **1a** and **2a** contain a distorted cubic $[M_4O_4]$-core, which is formed by μ_3-bridging oxygen atoms provided by the four phenolate residues of the diiminepyridine ligands (Figure 1b, thermal ellipsoids are presented in Figures 2 and 4 of the Supporting Information). The metal atoms are further coordinated to two chelating acetates in the equatorial planes and two bridging acetates in the axial positions. Two of the metal atoms are coordinated to four oxygen and three nitrogen atoms giving a distorted pentagonal bipyrimidal coordination sphere. The other two metal atoms are coordinated to only oxygen atoms leading to a distorted octahedral geometry. The overall neutrality of the cluster indicates that all four metals are in the +2 oxidation state.

Scheme 1. Tetranuclear Carboxylate Clusters Can Be Prepared via a Metal Template Reaction

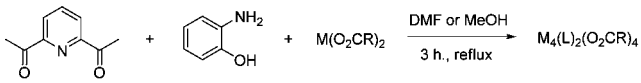

1a: M= Zn, R = CH_3
1b: M= Zn, R = C_6H_5
2a: M= Cd, R = CH_3
2b: M= Cd, R = C_6H_5

Exchange of the Carboxylate Ligand. A common method to alter the carboxylate ligand of a polynuclear cluster is by reaction of the cluster with a carboxylic acid,[25] although this does not always ensure complete replacement of the carboxylate ligand.[26] The addition of a slight excess of a methanolic benzoic acid solution to a stirring solution of $[Zn_4(L)_2(O_2CCH_3)_4]$ (**1a**) in methanol gives a crystalline precipitate. The poor solubility of the product hampers the growth of single crystals suitable for X-ray diffraction. The addition of a methanolic benzoic acid solution to a nonstirring solution of $[Zn_4(L)_2(O_2CCH_3)_4]$ (**1a**) leads to the formation of single crystals within 24 h (Table 1, thermal ellipsoids are presented in Figure 3 of the Supporting Information). The refinement of the crystal structure indicated an occupation of the disordered benzoate ligands of 66% compared to acetate (benzoate/acetate mean ratio of 2:1). The compound will be, for convenience, indicated with the molecular formula $[Zn_4(L)_2(O_2CCH_3)(O_2CC_6H_5)_3]$ (**1c**). Although a complete exchange of ligands was intended, this compound still proved to be useful as a reference compound for the intermolecular carboxylate exchange (*vide infra*).

Synthesis of $[M_4(L)_2(O_2CC_6H_5)_4]$ [M = Zn (1b), Cd (2b)]. To ensure a complete replacement of the carboxylate ligands, we prepared the tetranuclear carboxylate clusters via a direct method. The microcrystalline compounds $[M_4(L)_2(O_2CC_6H_5)_4]$ [M = Zn (**1b**) and Cd (**2b**)] precipitate from the template reaction between $M(O_2CC_6H_5)_2{\cdot}xH_2O$ (M = Cd or Zn), 2,6-diacetylpyridine, and 2-aminophenol in methanol. Unfortunately, the precipitated solids were not soluble enough for recrystallization to obtain single crystals, but their identity was unambiguously established via powder diffraction (see Supporting Information Figure 1) and confirmed by elemental analysis.

VT NMR of $[M_4(L)_2(O_2CCH_3)_4]$ [M = Zn (1a), Cd (2a)]. In Figure 2 the ^{1}H NMR spectra at 257, 298, and 357 K of $[Zn_4(L)_2(O_2CCH_3)_4]$ (**1a**) in DMF-d_7 are shown (for additional spectra, see Supporting Information Figure 9). The ^{1}H NMR spectrum at 298 K shows a very strong broadening of the peaks, indicative of dynamical processes within the tetranuclear cluster. Only proton 1 (see Figure 2 for the numbering of the protons) seems to be rather static; the peak is clearly resolved in a triplet with only minor broadening. The aromatic protons 2 and 4–7 between 6.3 and 8.3 ppm are very broad. The chemical shift of proton 3, attached to the methyl carbon atom on the imine, is in between the signals of the deuterated DMF solvent (around 2.8 ppm). The broad peaks at 1.36 and 0.82 ppm are assigned to the methyl group of the acetate ligands.

Upon heating the sample to 357 K the peaks become sharp and fully resolved. The spectrum shows a symmetrical diiminepyridine ligand, and the number of peaks are indicative of only one species in solution. Also, the two acetate peaks in the spectrum at 298 K have merged into a single peak at 1.25 ppm.

Cooling the sample from 298 to 257 K also leads to a sharpening and resolving of the peaks. The spectrum shows, however, the presence of an asymmetric diiminepyridine ligand. This asymmetry of the ligand implies that the tetranuclear

dx.doi.org/10.1021/ic401522v | *Inorg. Chem.* 2013, 52, 13004–13013

Table 1. Crystallographic Data and Structure Refinement Details of the Tetranuclear Clusters 1a, 1c, 2, 3, 4, and 5

	1a	1c	2a	3	4	5
formula	$C_{53}H_{58}N_6O_{15}Zn_4$	$C_{71}H_{58}N_6O_{14}Zn_4$	$C_{53}H_{55}Cd_4N_7O_{14}$	$C_{64}H_{72}Cl_6N_6O_{14}Zn_4$	$C_{32}H_{40}N_6O_9Zn_2$	$C_{50}H_{44}Cl_2N_6O_{12}Zn_4$
crystal color	yellow-brown	light brown-orange	red-brown	red-brown	orange-brown	orange translucent
M_w	1280.53	1480.71	1463.64	1623.46	783.44	1253.29
T (K)	98(2)	208(2)	98(2)	208(2)	208(2)	208(2)
radiation, λ (Å)	Mo Kα, 0.710 73	Mo Kα, 0.710 73	Mo Kα, 0.710 73	Mo Kα, 0.710 73	Mo Kα, 0.710 73	Mo Kα, 0.710 73
cryst syst	monoclinic	monoclinic	orthorhombic	monoclinic	monoclinic	orthorhombic
space group	$P2_1/n$	$P2_1/c$	$P2_12_12_1$	$P2_1/a$	$P2_1/n$	$Pccn$
a (Å)	11.3022(16)	16.3210(17)	14.3900(8)	14.5599(6)	8.8503(5)	11.3059(17)
b (Å)	22.274(4)	15.815(2)	16.1430(9)	15.9732(7)	24.955(3)	18.656(2)
c (Å)	21.923(3)	25.080(3)	23.611(3)	15.5271(16)	15.6176(19)	23.199(3)
α (deg)	90	90	90	90	90	90
β (deg)	103.818(10)	92.570(10)	90	104.473(6)	92.139(7)	90
γ (deg)	90	90	90	90	90	90
V (Å^3)	5359.2(15)	6467.0(14)	5484.9(8)	3496.5(4)	3446.9(6)	4893.3(11)
Z, D_{calcd} (mg/m^3)	4, 1.587	4, 1.521	4, 1.772	2, 1.542	4, 1.510	4, 1.701
GOF on F^2	1.133	1.062	1.092	1.031	1.075	1.157
final R1	0.0381	0.0648	0.0504	0.0605	0.1022	0.0872
wR2 [$I > 2\sigma(I)$]	0.0951	0.1351	0.0706	0.1500	0.2077	0.1948
R1, wR2 (all data)	0.0536, 0.1005	0.1234, 0.1566	0.1000, 0.0809	0.0854, 0.1676	0.1655, 0.2305	0.0939, 0.1912

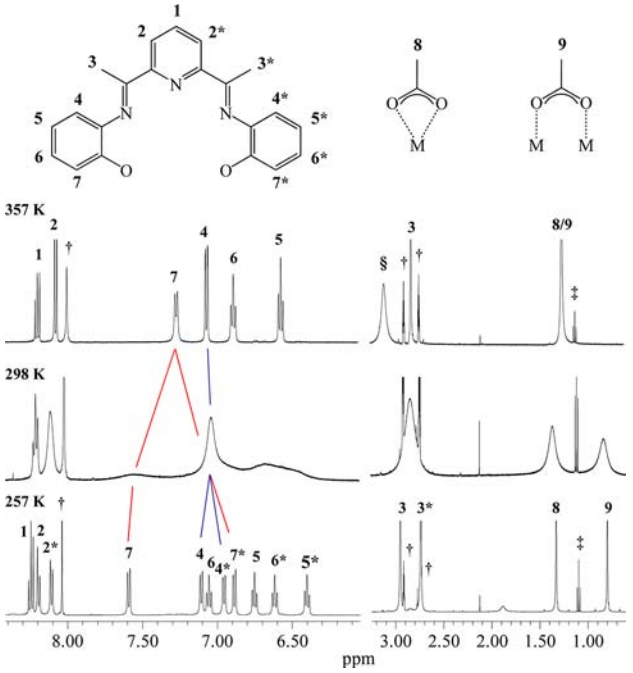

Figure 2. ^{1}H NMR spectrum of $Zn_4(L)_2(O_2CCH_3)_4$ (**1a**) in DMF-d_7 measured at three different temperatures. The * indicates that the corresponding proton atom is shielded by the aromatic system of the other ligand in the cluster. † = DMF-d_7 solvent peaks. ‡ = Trace amounts of Et_2O. § = MeOH solvent.

cluster is predominantly an intact cluster in solution, and the difference in chemical shift of the peaks within the same ligand is caused by a shielding effect caused by the other ligand. Because of the C_2 symmetry of the cluster as a whole, there is a distinction between signals from protons not related by 2-fold symmetry. A more descriptive way of explaining this asymmetry is by regarding the tetranuclear cluster as two equal moieties with the composition $M_2(L)(O_2CCH_3)_2$, of which the lowest part is rotated 90° with respect to the upper half. Half of the diiminepyridine ligand in the upper moiety is located above half of the diiminepyridine ligand of the lower part (schematically shown in Figure 5a, the S1 or S3 state).

These two "overlapping" parts of the diiminepyridine ligand are electronically influenced by each other, causing a different chemical shift in comparison with the noninteracting part of the diiminepyridine ligand. Hence, an asymmetrical diiminepyridine ligand is observed, when the dynamical behavior of the molecule becomes slower than the NMR time scale. At higher temperatures the dynamical behavior of the cluster is faster than the NMR time scale and the shielding effect is no longer observed. Furthermore, it is noticed that the chemical shift difference between the protons 4 and 4* ($\Delta\delta$ = 0.15 ppm) is much smaller than the chemical shift difference between protons 7 and 7* ($\Delta\delta$ = 0.71 ppm) (Table 2). The crystal

Table 2. Overview of the Chemical Shifts and Chemical Shift Differences of 1a and 2a

	1a (zinc cluster)			2a (cadmium cluster)		
proton no.	δ^a (357 K)	δ^a (257 K)	$\Delta\delta^{a,b}$	δ^a (357 K)	δ^a (257 K)	$\Delta\delta^{a,b}$
1	8.20	8.25		8.27	8.35	
2, 2*	8.08	8.20, 8.12	0.08	8.17	8.35, 8.20	0.15
3, 3*	2.82	2.96, 2.74	0.22	2.89	3.05, 2.77	0.28
4, 4*	7.06	7.11, 6.96	0.15	n.d.[c]	7.18, 7.04	0.14
5, 5*	6.56	6.76, 6.41	0.35	n.d.[c]	6.82, 6.39	0.43
6, 6*	6.88	7.06, 6.62	0.44	n.d.[c]	7.18, 6.67	0.51
7, 7*	7.26	7.60, 6.89	0.71	n.d.[c]	7.18, 6.55	0.63
8, 9	1.25	1.33, 0.80	0.53	1.31	1.44, 1.00	0.44

[a]The chemical shift is given in ppm. [b]The chemical shift difference is the difference within the asymmetric ligand or the difference between the carboxylate ligands at low temperature. [c]These peaks are very broad, and it is not possible to determine the exact chemical shift.

structure of the tetranuclear clusters shows a tilting of the phenolate moiety with regard to the pyridine ring (that is the nonplanarity of the N_3O_2 donor set). The position of proton 7 is closer to the aromatic system of the pyridine ring, and will therefore experience more shielding than proton 4. This shielding effect is seen for all the protons of the phenolate ring, with the difference between the proton and proton* (Figure 2)

dx.doi.org/10.1021/ic401522v | Inorg. Chem. 2013, 52, 13004−13013

increasing in the order of 7 > 6 > 5 > 4, which is a similar order as the distance from the proton to the aromatic system of the pyridine ring.

The two broad acetate peaks in the spectrum at 298 K become sharper at lower temperatures. The assignment of the peak at 1.33 ppm to the chelating carboxylate is based on the $^{13}C\{^1H\}$ NMR spectrum (see Supporting Information Figure 8) in combination with a COLOC spectrum. The bridging carboxylate ligand is assigned to the chemical shift at 0.80 ppm.

The ^1H NMR spectra of $[Cd_4(L)_2(O_2CCH_3)_4]$ (**2a**) at 257, 298, and 357 K are shown in Figure 3 (additional spectra can

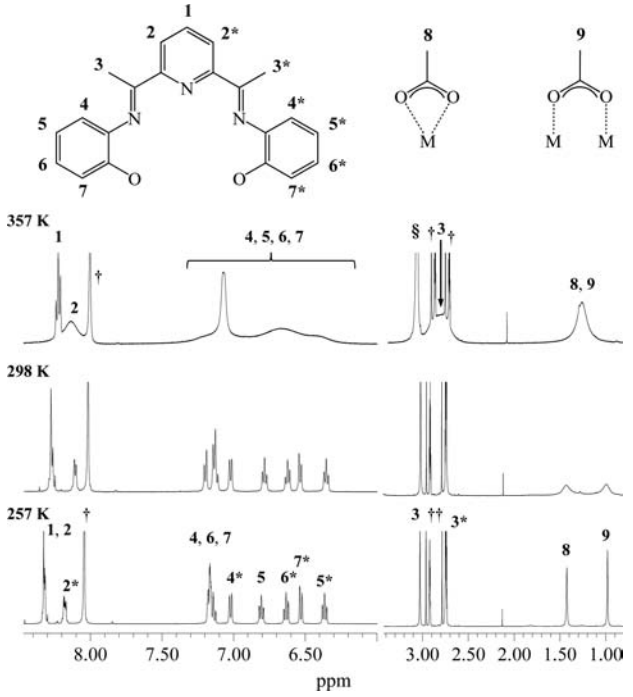

Figure 3. ^1H NMR spectrum of $Cd_4(L)_2(O_2CCH_3)_4$ (**2a**) in DMF-d_7 measured at three different temperatures. The * indicates that the corresponding proton atom is shielded by the aromatic system of the other ligand in the cluster. † = DMF-d_7 and DMF solvent peaks. § = H_2O present in the DMF-d_7 and solvent.

be found in the Supporting Information Figure 10). The ^1H NMR spectrum at 298 K of **2a** shows completely resolved and relatively sharp diiminepyridine signals, whereas these signals were already broadened for **1a** at this temperature. The spectrum of **2a** at 357 K strongly resembles with the spectrum of **1a** at 298 K, which means that the rate of this dynamical process is slower for the cadmium cluster than for the zinc cluster.

The number of signals in the spectrum of **2a** at 298 K belong to an asymmetric ligand, similar to the spectrum of **1a**. The two acetate signals of **2a**, at, respectively, 0.99 and 1.43 ppm, are still very broad at 298 K, similar to the room-temperature spectrum of **1a**. The coalescence temperature of the acetate signals of **2a** lies around 328 K (see Supporting Information Figure 10), which is at a higher temperature than the coalescence temperature of the acetate signals in **1a** (see Supporting Information Figure 9). This also indicates that the interconversion of chelating and *syn*–*syn* bridging carboxylate ligands is slower in the cadmium cluster **2a** than in the zinc cluster **1a**. The sharpness of the diiminepyridine signals and the broadness of the acetate peaks at 298 K indicate that these two dynamical processes are not highly correlated to one another. At a temperature of 357 K the acetate peaks have coalesced into a single peak, but this peak remains very broad.

The diiminepyridine signals are broadening upon increase of the temperature, except for the triplet of proton 1, which remains relatively sharp and resolved at 357 K. Lowering the temperature from 298 to 257 K does not alter much for the diiminepyridine signals compared to the room-temperature spectrum; they have some minor alterations in chemical shift and become sharper and more resolved. Again it can be seen that the protons, which experience more shielding from the pyridine ring, have larger chemical shift differences (Table 2). The $\Delta\delta$ between the signals of protons 4 and 4* is 0.14 ppm, which is similar to the value found for these proton signals in cluster **1a**. The value of the $\Delta\delta$ for the proton signals of 7 and 7* in cluster **2a** is 0.63 ppm, which is slightly smaller than the value found for these proton signals of cluster **1a**. The order of increasing $\Delta\delta$ is the same as seen within cluster **1a**. Lowering the temperature to 257 K sharpens the two acetate peaks. The assignment the spectrum was performed based on analogy with the zinc cluster **1a**.

Model and Thermodynamical Parameters for the Carboxylate Shift. The general exchange between *syn*–*syn* bridging and chelating carboxylate ligands is schematically represented in Figure 4. The VT ^1H NMR spectra of **1a** (see

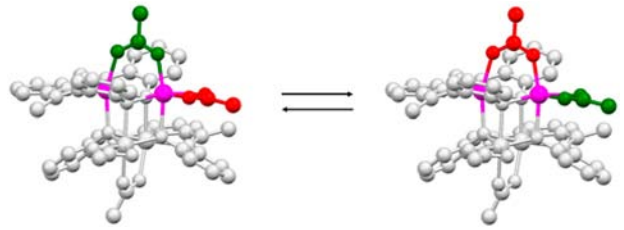

Figure 4. Schematic representation for the exchange of the carboxylate ligands. The chelating carboxylate changes to the bridging carboxylate and vice versa.

Supporting Information Figure 9) show that the two acetate peaks (0.80 and 1.33 ppm) at 257 K broaden and eventually merge when the temperature is increased. The coalescence temperature of these two peaks appears to be around 316 K. The Gibbs energy of activation ($\Delta G^{\ddagger}$) for this dynamical process is estimated to be 60.7 kJ/mol (Table 3). The value of $\Delta H^{\ddagger}$ is estimated to be 72 ± 5 kJ/mol and the value of $\Delta S^{\ddagger}$ to be 35 ± 16 J/(mol K) (Table 3). The analysis of the VT ^1H NMR spectra of **2a** (see Supporting Information Figure 10) show a slightly higher coalescence temperature for the acetate peaks, around 328 K. This corresponds with an estimated activation Gibbs energy of 57.6 kJ/mol. The Eyring plot (see Supporting Information Figure 14), based on the rate constant at different temperatures, leads to an estimation of $\Delta H^{\ddagger}$ of 43 ± 5 kJ/mol and a large negative $\Delta S^{\ddagger}$ of −63 ± 15 J/(mol K). Comparison with reported parameters of activation for the conversion of a $\mu_{1,2}$- to a $\mu_{1,1}$-coordination mode of carboxylate ligands in the compounds $[Zn_4(bdmap)_2(O_2CR)_6]$ (Hbdmap = 1,3-bis(dimethylamino)-2-propanol, R = Me or Et) showed comparable values of $\Delta G^{\ddagger}$ and $\Delta H^{\ddagger}$.[27] The reported value of $\Delta S^{\ddagger}$ for these compounds is strongly negative, and the authors ascribe this to intramolecular exchange. A negative value of $\Delta S^{\ddagger}$ implies that the transition state of the carboxylate exchange is more ordered than the ground state.[28] This would not be

dx.doi.org/10.1021/ic401522v | Inorg. Chem. 2013, 52, 13004−13013

Table 3. Activation Parameters for 1a and 2a Based on the VT NMR Spectra

	compd (no. of proton)					
param	**1a** (3)	**1a** (8,9)	**1a** (5)	**1a** (2)	**2a** (8,9)	**2a** (3)
$\Delta G^{\ddagger a,b}$	58.9	60.7	59.3	60.6	57.6	70.9
$\Delta H^{\ddagger a}$	66 ± 7	72 ± 5	*c*	*c*	43 ± 5	58 ± 6
$\Delta S^{\ddagger a}$	24 ± 24	35 ± 16	*c*	*c*	−63 ± 15	−35 ± 18

[a] $\Delta H^{\ddagger}$ and $\Delta G^{\ddagger}$ values are given in kJ/mol, $\Delta S^{\ddagger}$ values are given in J/(mol K). [b] Estimated error 10%. [c] Insufficient data points for an Eyring plot.

achieved by intermolecular exchange, because the carboxylate ligand then has to dissociate from the tetranuclear cluster (under the assumption that an associative mechanism is not occurring). Similar values are found for the interconversion of *syn*−*syn*-$\mu_{1,3}$- to *syn*−*anti*-$\mu_{1,1}$-carboxylate ligands in carbamatomagnesium bromides.[28] The activation entropy of the carboxylate exchange in the tetranuclear cadmium cluster **2a** is strongly negative (Table 3 and Supporting Information Figure 13), which suggests an intramolecular exchange process.

Proposed Model for the Inversion of Chirality of the Clusters: Nondissociative. In Figure 5a, a schematic

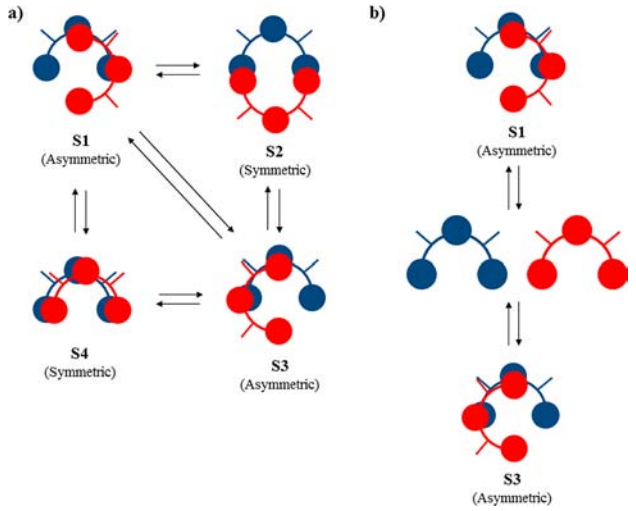

Figure 5. Possible mechanisms of the dynamics, observed for the diiminepyridine ligand, are (a) the cluster remains intact and the two halves rotate around each other, and (b) the cluster dissociates into two dinuclear moieties.

representation of the first model is shown. The model comprises a nondissociative mechanism, which starts with one of the chiral conformations of the tetranuclear cluster (denoted with S1 in Figure 5a). The tetranuclear cluster is represented by the two diiminepyridine ligands, of which one ligand is rotated 90° with respect to the other ligand. Assuming, for convenience, that the "blue" ligand has a static position, the "red" ligand is rotating around the axial bonds in the plane above. Rotation of the "red" ligand over 90° leads either to conformation S2 or S4 depending on the direction of rotation. In the S4 state the two diiminepyridine ligands are positioned above each other, which could lead to steric hindrance of the substituents on the imine. It is more likely that the "red" diiminepyridine ligand will rotate in the other direction to form S2. This S2 intermediate seems to be trapped in the crystal structure of $Zn_4(L2)_2(O_2CCH_3)_4$ (**3**) ($L2H_2$ = 2,6-bis(4-*tert*-butyl-6-(methylidenylamino)phenol)pyridine) (see Figure 6) (Table 1) (ORTEP representation is given in the Supporting Information Figure 5). Compared with the cubane structure of

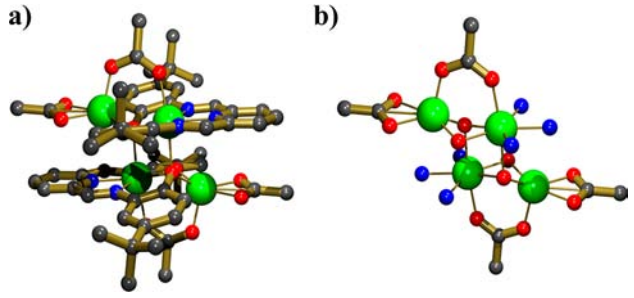

Figure 6. (a) Crystal structure of $[Zn_4(L2)_2(O_2CCH_3)_4]$ (**3**) ($L2H_2$ = 2,6-bis(4-*tert*-butyl-6-(methylidenylamino)phenol)pyridine). (b) Crystal structure of $[Zn_4(L2)_2(O_2CCH_3)_4]$ (**3**) without the ligand L2 to give a better view of the metal−oxygen core: zinc, green; oxygen, red; nitrogen, blue; carbon, gray; coordination and covalent bond, bronze. Hydrogen atoms and solvent molecules are omitted for clarity.

1a and **2a**, two of the μ_3-bridging oxygen atoms have become μ_2-briding atoms, giving a stepped-cubane structure.[29] This geometry could potentially serve as the intermediate S2 in our intramolecular conversion of the tetranuclear clusters. A second rotation over 90° leads to state S3, which is in principle identical to S1. The difference between S1 and S3 is the handedness of the compound, illustrated in Figure 7 with

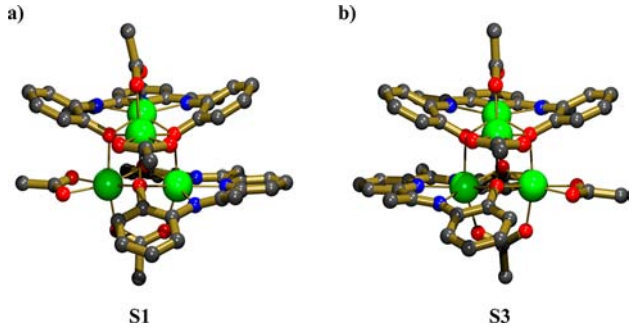

Figure 7. The two conformations of the tetranuclear carboxylate cluster: (a) the S1 conformation, (b) the S3 conformation.

crystal structures of the two chiral forms. In general, according to this model the dynamical process described by the cluster would be a nondissociative conversion of one stereoisomer to the other stereoisomer.

Thermodynamical Parameters for the Inversion of Chirality of the Clusters. The ^1H NMR spectra at low temperatures of compounds **1a** and **2a** show only peaks corresponding to an asymmetric diiminepyridine ligand, which corresponds to the presence of an intact tetranuclear cluster in solution. It is very difficult to estimate the precise activation parameters for this process, since many peaks are overlapping and the coalescence points cannot be precisely determined. The methyl groups on the imine give peaks which partially overlap with the DMF solvent peaks, but still an estimation of the

activation parameters can be obtained. In compound **2a** the coalescence temperature of the methyl peaks is estimated at 357 K, which corresponds with $\Delta G^{\ddagger}$ = 70.9 kJ/mol (Table 3). With estimated rate constants at other temperatures, an Erying plot is constructed (see Supporting Information Figure 13), which gives values of $\Delta H^{\ddagger}$ = 58 ± 6 kJ/mol and $\Delta S^{\ddagger}$ = −35 ± 18 J/(mol K). A negative value of $\Delta S^{\ddagger}$ implies that the transition state of the exchange is more ordered than the ground state,[28] which is in favor of the first possible model proposed in Figure 5a. The activation parameters for the methyl protons of **1a** are a bit more difficult to determine due to the severe overlap with the DMF solvent peaks. The VT ^{1}H NMR spectra in Supporting Information Figure 9 show that the coalescence temperature lies probably between 292 and 298 K and is, therefore, estimated at 295 K. The activation Gibbs energy is estimated at 58.9 kJ/mol, which is smaller than the value found for compound **2a**. The values of $\Delta H^{\ddagger}$ and $\Delta S^{\ddagger}$ have been estimated to be, respectively, 66 ± 7 kJ/mol and 24 ± 24 J/(mol K) with the aid of an Eyring plot (see Supporting Information Figure 13). The activation entropy is difficult to interpret, because of the large error. It was possible to determine the Gibbs activation energy for two other protons of the diiminepyridine ligands, as given in Table 3. The values of $\Delta G^{\ddagger}$ for protons 5 and 2 are, respectively, 59.3 and 60.6 kJ/mol, which correspond well with the value found for proton 3 of this compound.

Proposed Model for the Inversion of Chirality of the Clusters: Dissociative. The second possible model for the dynamical process of the diiminepyridine ligand is the dissociation of the cluster into two $[M_2(L)(O_2CR)_2]$ moieties (schematically shown in Figure 5b), which then form an equilibrium. The low-temperature ^{1}H NMR spectra for compounds **1a** and **2a** give no indication of large amounts of dissociated tetranuclear cluster. If dissociation was occurring on an NMR slow time scale, one would expect to see half cluster. Furthermore, this dissociation would mean that the axial M−O bonds in solution are very weak, but the bond lengths in the solid state [for cluster **1a** in the range 2.1588(19)−2.1956(19) Å and for cluster **2a** in the range 2.311(3)−2.548(3) Å] are typical M−O bonds, indicating a certain strength of these bonds. Yet, a $[M_2(L)(O_2CR)_2]$ moiety was isolated from the reaction of $Zn(O_2CCH_3)_2{\cdot}2H_2O$, 2,6-diformylpyridine and 2-amino-phenol. The crystal structure of $Zn_2(L3)(O_2CCH_3)_2(DMF){\cdot}2DMF$ (**4**) [$L3H_2$ = 2,6-bis(2-hydroxyphenylimino-methyl)pyridine, Figure 8] demonstrates the existence of a semicluster as proposed in Figure 5b.

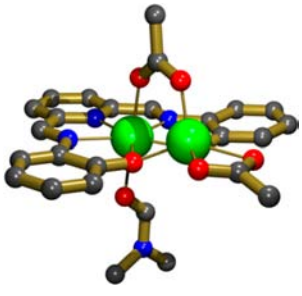

Figure 8. (a) Crystal structure of $Zn_2(L3)(O_2CCH_3)_2(DMF){\cdot}2DMF$ (**4**) ($L3H_2$ = 2,6-bis(4-*tert*-butyl-6-(methylidenylamino)-phenol)-pyridine). Hydrogen atoms and solvent molecules are omitted for clarity: zinc, green; oxygen, red; nitrogen, blue; carbon, gray; coordination and covalent bond, bronze.

Dissociation of Tetranuclear Clusters. To investigate the possibility of the dissociative mechanism, NMR experiments with a mixture of two tetranuclear zinc clusters with different diiminepyridine ligands were performed. One could expect an superposition of the signals of the individual compounds in the ^{1}H NMR spectrum if the cluster does not dissociates in solution. If scrambling of the diiminepyridine ligands does occur, one can expect new peaks to arise at (slightly) different chemical shifts. In Figure 9a, a part of the ^{1}H NMR spectrum of

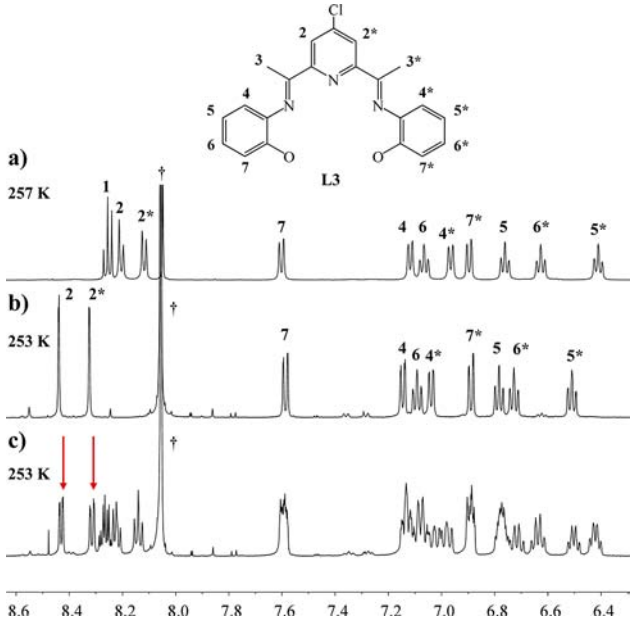

Figure 9. ^{1}H NMR spectrum in DMF-d_7 of (a) $[Zn_4(L)_2(O_2CCH_3)_4]$ (**1a**) at 253 K, (b) $[Zn_4(L3)_2(O_2CCH_3)_4]$ (**5**) at 253 K, and (c) 1:1 mixture of $[Zn_4(L)_2(O_2CCH_3)_4]$ (**1a**) and $[Zn_4(L3)_2(O_2CCH_3)_4]$ (**5**) at 253 K. † = DMF-d_7 solvent peaks. The peaks, indicated with red arrows, show most clearly the presence of a mixed tetranuclear compound with the composition $[Zn_4(L)(L3)(O_2CCH_3)_4]$.

$[Zn_4(L)_2(O_2CCH_3)_4]$ (**1a**) at 257 K is shown, which has been discussed earlier in this Article. The ^{1}H NMR spectrum of $[Zn_4(L3)_2(O_2CCH_3)_4]$ (**5**) ($L3H_2$ = 2,6-bis(1-(2-hydroxyphenyl)-iminoethyl)4-chloropyridine) (see Supporting Information Figure 7 for an ORTEP representation of this cluster) at 253 K is given in Figure 9b. The protons $4^{(*)}$−$7^{(*)}$ of cluster **5** have nearly the same chemical shifts as the same protons in cluster **1a**. A distinct difference between the two clusters can be found at the signals of protons 2 and 2*, which are much more downfield for cluster **5**. In Figure 9c the ^{1}H NMR spectrum of a 1:1 mixture of clusters **1a** and **5** after 24 h in DMF-d_7 solution is presented. The spectrum contains the signals corresponding to the clusters **1a** and **5**, meaning that these clusters are still present in solution. However, also signals with slight chemical shift compared to the original clusters have appeared. This is most clearly visible for protons 2 and 2* of the ligand L3 (indicated with red arrows). This means that scrambling of the ligands can also occur in solution and that the clusters can dissociate and reassemble to form $[Zn_4(L)(L3)(O_2CCH_3)_4]$.

Variable-Temperature NMR of Benzoate Complexes $[M_4(L)_2(O_2CC_6H_5)_4]$ [M = Zn (1b), Cd (2b)]. Upon going from an acetate to a benzoate ligand, the rate of the chemical exchange alters. The ^{1}H NMR spectrum of $[Cd_4(L)_2(O_2CC_6H_5)_4]$ (**2b**) at 293 K shows broad benzoate

dx.doi.org/10.1021/ic401522v | *Inorg. Chem.* 2013, 52, 13004−13013

ligand resonances (Figure 10), similar to the acetate signals of **2a** around this temperature. The resonances of the protons of

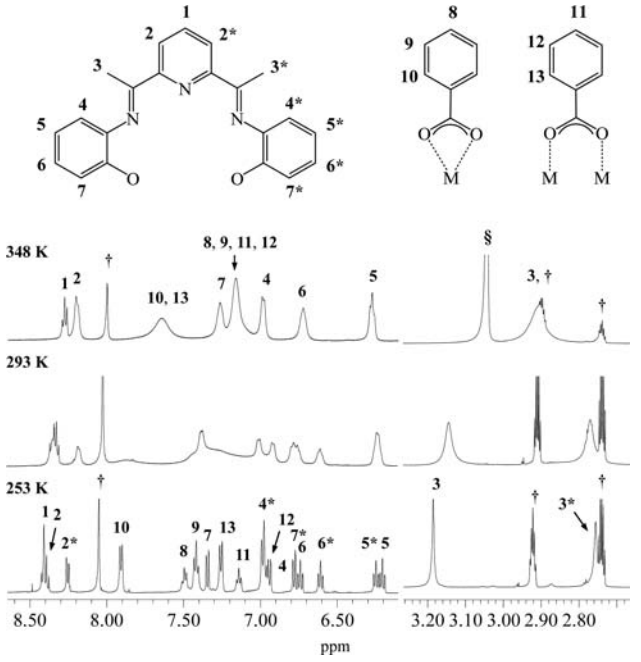

Figure 10. ^{1}H NMR spectrum of $Cd_4(L)_2(O_2CC_6H_5)_4$ (**2b**) in DMF-d_7 measured at three different temperatures. The * indicates that the corresponding proton atom experiences a shielding effect by the aromatic system of the other ligand in the cluster. † = DMF-d_7 solvent peaks. § = H_2O present in the DMF-d_7.

the diiminepyridine ligand are broad, but slightly resolved at 293 K. The coalescence temperature of these signals lies at a much lower temperature than the coalescence temperature of the diiminepyridine ligand within cluster **2a**. This means that the rate of the chemical exchange of **2b** has become faster compared to **2a**. Increasing the temperature to 348 K causes the diiminepyridine protons to coalesce, but the peaks are still broadened (see Supporting Information Figure 12). The benzoate protons also coalesce to single peaks belonging to each of the coordination modes, but these peaks remain broad at this high temperature. Decreasing the temperature from 293 to 253 K shows a spectrum with an asymmetric diiminepyridine ligand, which means that the compound is predominantly in the S1 or S3 state (Figure 5) in solution. The assignment of the sharp and resolved peaks was achieved with the aid of COSY. Remarkably, not all phenolate protons are affected in the same way by the shielding of the aromatic pyridine ring, as can be seen by comparison of protons 4 and 4* with 7 and 7* (Table 4). The chemical shift of 7* is more upfield than the chemical shift of 7, whereas the COSY indicates that this is reversed for proton 4 (4 lies more upfield than 4*). This can be explained by the chelating carboxylate ligand, which itself can cause also a shielding effect.

The proton 7* is shielded by the aromatic pyridine ligand, whereas proton 7 is shielded by the chelating benzoate ligand. Also for proton 4* the shielding is caused by the aromatic pyridine ring, while the shielding of proton 4 is caused by the chelating benzoate ligand. The effect of the chelating benzoate ligand is for proton 4 apparently large enough to shift this peak upfield compared to 4*. For proton 7 and 7* this reversal in chemical shift is not observed, because the effect of the

Table 4. Chemical Shifts and Chemical Shift Differences of the Asymmetric Diiminepyridine Ligand of 1b and 2b

	1b (zinc cluster)			**2b** (cadmium cluster)		
proton no.	$\delta^{a,b}$ (331 K)	δ^a (243 K)	$\Delta\delta^a$	δ^a (348 K)	δ^a (248 K)	$\Delta\delta^a$
1	8.36	8.35		8.28	8.42	
2, 2*	8.22	8.30, 8.26	0.04	8.21	8.39, 8.27	0.12
3, 3*	2.89	n.d.[d]		2.91	3.19, 2.75	0.44
4, 4*	7.08	6.90, 6.90	(−) 0.0[e]	6.99	7.96, 7.95	−0.01[c]
5, 5*	6.38	6.23, 6.17	−0.06[e]	6.28	6.25, 6.20	−0.05[c]
6, 6*	6.88	6.72, 6.61	0.11	6.72	6.74, 6.61	0.13
7, 7*	7.47	7.81, 7.24	0.57	7.27	7.34, 6.78	0.56
8, 11	7.21	7.48, 6.90	0.42	7.16	7.50, 7.15	0.35
9, 12	7.21	7.40, 6.90	0.50	7.16	7.42, 6.98	0.44
10, 13	7.71	7.90, 7.08	0.82	7.64	7.91, 7.26	0.65

[a]The chemical shift is given in ppm. [b]Measured at 200 MHz NMR. [c]The peaks have reversed in order; that is, the asterisk indicates a peak that is more downfield. [d]The assignment of these protons was not conclusive. [e]The order of the peaks is reversed in comparison with the other peaks.

shielding from the pyridine ligand is much larger. The $\Delta\delta$ between the protons 4 and 4* ($\Delta\delta$ = 0.01 ppm) is very small, and much smaller than the $\Delta\delta$ between protons 7 and 7* ($\Delta\delta$ = 0.56 ppm) (Table 4). The order of increasing $\Delta\delta$ is the same as seen with the clusters **1a** and **2a**. The overlapping peaks in this spectrum make it impossible to determine the coalescence temperature of the different protons, and hence, it is not possible to estimate the parameters of activation. The low-temperature NMR spectrum resembles the low-temperature spectra of the compounds **2a** and **1a** which again implies a nondissociative mechanism of rotation of the diiminepyridine ligands (Figure 5a).

The ^{1}H NMR spectrum of $[Zn_4(L)_2(O_2CC_6H_5)_4]$ (**1b**) at 298 K shows very broad peaks, which cannot be fully assigned (Figure 11). This spectrum is comparable with the spectra of **1a** and **2a** at this temperature. Changing the carboxylate ligand (from acetate to benzoate) for the cadmium clusters induces a change in chemical exchange rate (with benzoate the rate becomes slower), whereas this change in carboxylate ligand for the zinc clusters has no distinct effect on the chemical exchange rate. Increasing the temperature to 331 K leads to a sharpening of the signals (see Supporting Information Figure 11) and indicates a symmetric diiminepyridine ligand. The peaks are not completely resolved, and remain relatively broad at this temperature. Upon lowering the temperature a very complex spectrum was observed with too many peaks even for an asymmetric ligand. However, upon a closer inspection of the spectrum several features can be extracted. This is best seen at the peaks of protons 1 and 2$^{(*)}$ as visualized in the enlarged part of the aromatic system in Figure 11b. In the area around 8.5 ppm there are two triplets and three doublets present. The integral of the peaks is consistent with a distribution of one symmetrical and one asymmetrical diiminepyridine ligand, which means that, besides a tetranuclear cluster, another species is present in the solution, which exchanges with the tetranuclear

dx.doi.org/10.1021/ic401522v | Inorg. Chem. 2013, 52, 13004−13013

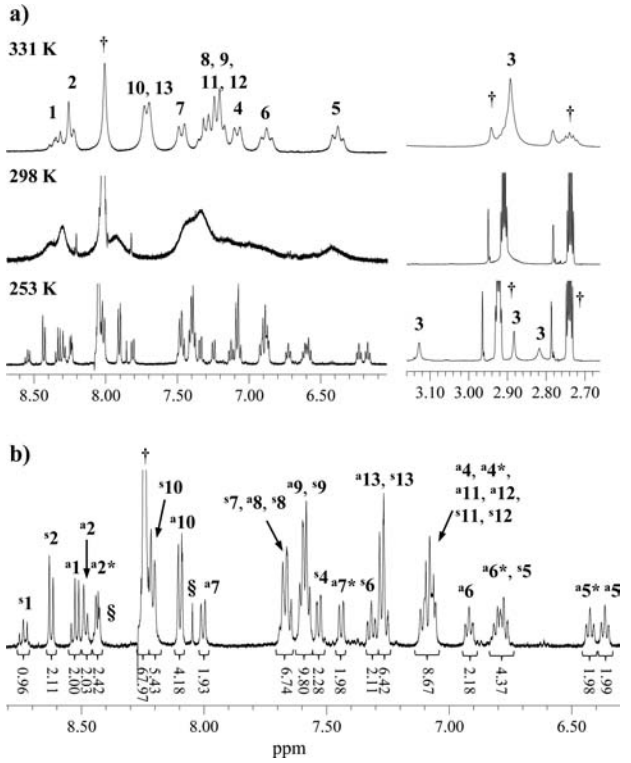

Figure 11. (a) ^{1}H NMR spectrum at 253, 298, and 331 K and the assignment of the peaks in the phenyl region of **1b**. The * indicates that the corresponding proton is shielded by the aromatic system of the other ligand in the cluster. † = DMF-d_7 solvent peaks.

cluster. The possible nature of this symmetrical species is discussed *vide infra*. In the asymmetric ligand the protons of the phenolate moiety are again either shielded by the pyridine ring of the ligand or by the chelating benzoate ligand. This is reflected in the chemical shifts of the different protons. Assuming that 7* (shielded by the pyridine ring) lies more upfield than 7, it is seen that this is reversed for proton 5. This is also reversed for proton 4, as indicated by the COSY spectrum, but this cannot be seen in Figure 11b due to the overlap with other peaks. There is almost no difference between the chemical shifts of proton 4 and 4* ($\Delta\delta$ = 0.0 ppm), similar to that in compound **2b** (Table 4). Also, the chemical shift difference between 7 and 7* ($\Delta\delta$ = 0.57 ppm) is comparable to the chemical shift difference observed for these protons in **2b**. The chemical shift differences within the compounds **1b** and **2b** are similar to each other, whereas in the compounds **1a** and **2a** there was a clear difference in these values. The VT ^{1}H NMR spectra of **1b** and **2b** are very similar in that they have both broad peaks at room temperature and at high temperatures.

The ^{1}H NMR spectra at low temperatures of tetranuclear cluster **1b** shows a combination of peaks attributed to an asymmetric and a symmetric diiminepyridine ligand. The observation of these two types of diiminepyridine ligands could be explained with both suggested models. In model one the conversion of the S1 conformation to the S3 conformation has to proceed via either S2 or S4 as an intermediate which are both symmetrical. Of these two intermediate states, the S2 state is perhaps the most likely intermediate, because of the less sterically hindered coordination of the ligands. The ratio between the asymmetric and the symmetric ligand in the ^{1}H NMR spectrum is 2:1. This could mean that the states S1, S2, and S3 are present in equal amounts in solution (S1 and S3 give the same spectrum). It has to be said, however, that these compounds should also be an intermediate for the dynamics in compounds **1a**, **2a**, and **2b**, but no peaks were observed in the ^{1}H NMR spectrum, which corresponds to this intermediate. This intermediate species which arises from exchanging the carboxylate ligand from acetate to benzoate suggests that the Zn−O−Zn bond is weakened. It suggests that the two exchange mechanisms are interrelated. The dissociation of the tetranuclear cluster, as suggested in model two (Figure 5b), gives a "semi"-cluster, in which the ^{1}H NMR spectrum would lead to a symmetric diiminepyridine ligand. In this "semi"-cluster there are still two different types of carboxylate ligands present, which would give two sets of benzoate peaks in the NMR (as is observed). The observed ratio between asymmetric and symmetric ligand in the ^{1}H NMR spectrum of 2:1 would mean that only part of the compound is dissociated in solution and that the majority is still a tetranuclear cluster.

Intermolecular Carboxylate Exchange. The thermodynamical parameters of the carboxylate dynamics in compound **1a** and **2a** are contradictory regarding this process being inter- or intramolecular (Table 3). To find out whether intermolecular carboxylate exchange is occurring for our cluster, we measured the ^{1}H NMR spectrum of a 1:1 mixture of **1a**/**1b** (zinc acetate and benzoate clusters) and **2a**/**2b** (cadmium acetate and benzoate clusters). If there is no intermolecular exchange between the carboxylate ligands, a ^{1}H NMR spectrum of the two individual compounds is expected. The obtained spectra are compared to the spectrum of $[Zn_4(L)_2(O_2CCH_3)(O_2CC_6H_5)_3]$ (**1c**) (the synthesis of this compound was discussed in the beginning of this Article). This type of exchange of carboxylate ligands between carboxylate clusters has been observed for the mixing of derivatives of the well-known Mn^{12}-cluster.[30]

The low-temperature ^{1}H NMR spectrum of compound **1c** is very complex, as can be seen in Figure 12a. It was not possible to fully assign all peaks, but the peaks in two regions (red and blue circle) can provide information about the different species.

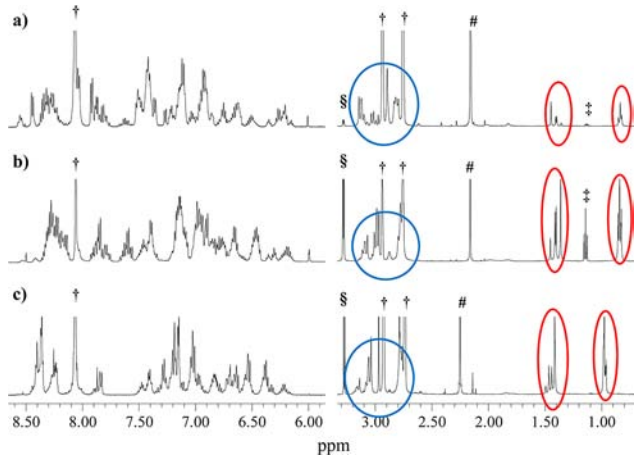

Figure 12. ^{1}H NMR spectra in DMF-d_7 of (a) $[Zn_4(L)_2(O_2CCH_3)(O_2CC_6H_5)_3]$ (**1c**) at 243 K. (b) 1:1 mixture of $[Zn_4(L)_2(O_2CCH_3)_4]$ (**1a**) and $[Zn_4(L)_2(O_2CC_6H_5)_4]$ (**1b**). (c) 1:1 mixture of $[Cd_4(L)_2(O_2CCH_3)_4]$ (**2a**) and $[Cd_4(L)_2(O_2CC_6H_5)_4]$ (**2b**). The acetate resonance peaks are highlighted by the red circle and the methyl substituent on the imine with blue circles. † = DMF-d_7 solvent peaks. # = residual acetone solvent peak. ‡ = residual diethylether solvent peak.

dx.doi.org/10.1021/ic401522v | *Inorg. Chem.* 2013, 52, 13004−13013

The bridging acetate peaks are found around 0.79 ppm, and these peaks have chemical shifts close to each other, leading to a significant amount of overlap. The chelating acetate has chemical shifts around 1.35 ppm, and these are more spread in chemical shift. There are four chelating acetate signals visible, differing in intensity, indicating that there is a statistical mixture present in solution. This mixture contains presumably all possible combinations: $[Zn_4(L)_2(O_2CCH_3)(O_2CC_6H_5)_3]$, $[Zn_4(L)_2(O_2CCH_3)_2(O_2CC_6H_5)_2]$, $[Zn_4(L)_2(O_2CCH_3)_3(O_2CC_6H_5)]$, and $[Zn_4(L)_2(O_2CCH_3)_4]$.[31] Of course, the compound $[Zn_4(L)_2(O_2CC_6H_5)_4]$ is also present in solution, but it does not have any acetate ligand and thus cannot be identified from this ^{1}H NMR spectrum. The multiple methyl resonances in the area around 3.0 ppm show that the compounds in solution are asymmetric and therefore indicate that nearly all compounds in solution are tetranuclear clusters.

The ^{1}H NMR spectrum of a 1:1 mixture of $[Zn_4(L)_2(O_2CCH_3)_4]$ (**1a**) and $[Zn_4(L)_2(O_2CC_6H_5)_4]$ (**1b**) (Figure 12b) clearly shows that intermolecular exchange of carboxylate ligands is occurring and that a statistical mixture of the different compounds is formed. The distribution between the different compounds is different as seen in the ^{1}H NMR spectrum for $[Zn_4(L)_2(O_2CCH_3)(O_2CC_6H_5)_3]$ (**1c**).

A similar ^{1}H NMR spectrum was measured from a 1:1 mixture of the clusters $[Cd_4(L)_2(O_2CCH_3)_4]$ (**2a**) and $[Cd_4(L)_2(O_2CC_6H_5)_4]$ (**2b**) (Figure 12c). The methyl resonances around 3.0 ppm also indicate that the majority of the species in solution contain an asymmetric diiminepyridine ligand and that the compounds are tetranuclear clusters in solution. There are four resonances around 1.45 ppm, which are attributed to the chelating acetate ligands. Furthermore, these peaks have the same intensity distribution as was seen in the mixture of the zinc clusters (Figure 12b,c). There is clearly a preference, as seen by the distribution, for the acetate over benzoate ligands. These experiments do, however, show that the carboxylate ligands are not fixed to a particular cluster, but that they readily interchange between different clusters. The activation parameters for this carboxylate exchange, as estimated from the ^{1}H NMR spectra, showed that this process is intramolecular for compound **2a** ($\Delta S^{\ddagger} = -63 \pm 15$ J/mol K). This is different with exchange experiments for **1a**, which show a positive value of $\Delta S^{\ddagger}$ (=35 ± 16 J/mol K). One could conclude that the carboxylate shift is both an inter- as well as an intramolecular exchange process, but that this is for the zinc clusters (**1a** and **1b**) predominantly intermolecular, whereas for the cadmium clusters (**2a** and **2b**) this is probably predominantly intramolecular.

CONCLUSION

Zinc and cadmium tetranuclear carboxylate clusters with either acetate or benzoate ligands were studied by VT ^{1}H NMR solution spectroscopy. It was shown that the dynamics can be described by two apparently uncorrelated processes: the carboxylate exchange and the diiminepyridine ligand rotation. Experimentally it was determined that the interconversion between chelating and *syn*−*syn* bridging carboxylate ligands occurs both intra- as well as intermolecularly. The thermodynamical parameters derived from the VT ^{1}H NMR spectra suggests for $[Zn_4(L)_2(O_2CCH_3)_4]$ (**1a**) that the exchange mechanism is predominantly intermolecular. For $[Cd_4(L)_2(O_2CCH_3)_4]$ (**2a**) these parameters suggest a more intramolecular interconversion of the carboxylate ligands. Clearly, the change in metal for the cluster has a strong influence on the dynamical behavior of the carboxylate ligands. For the dynamical process, which involves the diiminepyridine ligand, two possible models are discussed. Estimated activation parameters for compounds **2a** and **1a** suggest that the dynamics are even more complex and that this process is nondissociative, which supports the first model. Scrambling experiments show that the tetranuclear carboxylate cluster can dissociate in solution, which is in favor of the second model. Crystal structures support both the nondissociative and dissociative processes for the diiminepyridine ligand. We feel that these results reveal that these cubic metal clusters are surprisingly dynamic and that insight into these dynamic processes may help to explain the properties of related biological systems.

ASSOCIATED CONTENT

Supporting Information

Experimental procedures, crystallographic data (CIF), and additional NMR spectroscopy data. This material is available free of charge via the Internet at http://pubs.acs.org.

AUTHOR INFORMATION

Corresponding Author

*E-mail: a.rowan@science.ru.nl.

Notes

The authors declare no competing financial interest.

REFERENCES

(1) (a) Kok, B.; Forbush, B.; McGloin, M. *Photochem. Photobiol.* **1970**, *11*, 457. (b) Klein, M. P.; Sauer, K.; Yachandra, V. K. *Photosynth. Res.* **1993**, *38*, 265. (c) Messinger, J.; Robblee, J. H.; Bergmann, U.; Fernandez, C.; Glatzel, P.; Visser, H.; Cinco, R. M.; McFarlane, K. L.; Bellacchio, E.; Pizarro, S. A.; Cramer, S. P.; Sauer, K.; Klein, M. P.; Yachandra, V. K. *J. Am. Chem. Soc.* **2001**, *123*, 7804. (d) Ferreira, K. N.; Iverson, T. M.; Maghlaoui, K.; Barber, J.; Iwata, S. *Science* **2004**, *303*, 1831. (e) Loll, B.; Kern, J.; Saenger, W.; Zouni, S.; Biesiadka, J. *Nature* **2005**, *438*, 1040. (f) Mukhopadhyay, S.; Mandal, S. K.; Bhaduri, S.; Armstrong, W. H. *Chem. Rev.* **2004**, *104*, 3981. (g) Barber, J. *Chem. Soc. Rev.* **2009**, *38*, 185.

(2) (a) Affronte, M.; Troiani, F.; Ghirri, A.; Carretta, S.; Santini, P.; Corradine, V.; Schuecker, R.; Muryn, C.; Timco, G.; Winpenny, R. E. *Dalton Trans.* **2006**, *23*, 2810. (b) Wernsdorfer, W. *Int. J. Nanotechnol.* **2010**, *7*, 479. (c) Leuenberger, M. N.; Loss, D. *Nature* **2001**, *410*, 789. (d) Ardavan, A.; Rival, O.; Morton, J. J. L.; Blundell, S. J. *Phys. Rev. Lett.* **2007**, *98*, 057201.

(3) (a) Rardin, R. L.; Tolman, W. B.; Lippard, S. J. *New J. Chem.* **1991**, *15*, 417. (b) Wallar, B. J.; Lipscomb, J. D. *Chem. Rev.* **1996**, *96*, 2625. (c) Solomon, E. I.; Brunold, T. C.; Davis, M. I.; Kemsley, J. N.; Lee, S.-K.; Lehnert, N.; Neese, F.; Skulan, A. J.; Yang, Y.-S.; Zhou, J. *Chem. Rev.* **2000**, *100*, 235. (d) Weston, J. *Chem. Rev.* **2005**, *105*, 2151. (e) Parkin, G. *Chem. Rev.* **2004**, *104*, 699. (f) Maret, W.; Li, Y. *Chem. Rev.* **2009**, *109*, 4682.

(4) Lippard, S. J. *Carboxypeptidase A and Thermolysin: Structural Studies*; University Science Books: Mill Valley, CA, 1994.

(5) Ryde, U. *Biophys. J.* **1999**, *77*, 2777.

(6) (a) Torrent, M.; Musaev, D. G.; Basch, H.; Morokuma, K. *J. Comput. Chem.* **2002**, *23*, 59. (b) Andersson, M. E.; Hoegbom, M.; Rinaldo-Matthis, A.; Andersson, K. K.; Sjoeberg, B.-M.; Nordlund, P. *J. Am. Chem. Soc.* **1999**, *121*, 2346. (c) Voegtli, W. C.; Khidekel, N.; Baldwin, J.; Ley, B. A.; Bollinger, J. M., Jr.; Rosenzweig, A. C. *J. Am. Chem. Soc.* **2000**, *122*, 3255. (d) Herold, S.; Lippard, S. J. *J. Am. Chem. Soc.* **1997**, *119*, 145. (e) Torrent, M.; Mogi, K.; Basch, H.; Musaev, D. G.; Morokuma, K. *J. Phys. Chem. B* **2001**, *105*, 8616. (f) LeCloux, D. D.; Barrios, A. M.; Mizoguchi, T. J.; Lippard, S. J. *J. Am. Chem. Soc.* **1998**, *120*, 9001.

(7) (a) Sousa, S. F.; Fernandes, P. A.; Ramos, M. J. *Chem.—Eur. J.* **2009**, *15*, 4243. (b) Sousa, S. F.; Fernandes, P. A.; Ramos, M. J. *Bioorg.*

Med. Chem. **2009**, *17*, 3369. (c) Sousa, S. F.; Fernandes, P. A.; Ramos, M. J. *J. Am. Chem. Soc.* **2007**, *129*, 1378. (d) Sousa, S. F.; Fernandes, P. A.; Ramos, M. J. *Biophys. J.* **2005**, *88*, 483.

(8) (a) Park, H.-W.; Boduluri, S. R.; Moomaw, J. F.; Casey, P. J.; Beese, L. S. *Science* **1997**, *275*, 1800. (b) Long, S. B.; Casey, P. J.; Beese, L. S. *Biochemistry* **1998**, *37*, 9612. (c) Dunten, P.; Kammlott, U.; Crowther, R.; Weber, D.; Palermo, R.; Birktoft, J. *Biochemistry* **1998**, *37*, 7907.

(9) Tobin, D. A.; Pickett, J. S.; Hartman, H. L.; Fierke, C. A.; Penner-Hahn, J. E. *J. Am. Chem. Soc.* **2003**, *125*, 9962.

(10) Mujika, J. I.; Mulholland, A. J.; Harvey, J. N. In *Computational Inorganic Bioinorganic Chemistry*; Solomon, E. I., Scott, R. A., King, R. B., Eds.; WILEY-VCH: Weinheim, 2009; p 343.

(11) (a) Parrilha, G. L.; Fernandes, C.; Bortoluzzi, A. J.; Szpoganicz, B.; Silva, M. d. S.; Pich, C. T.; Terenzi, H.; Horn, A., Jr. *Inorg. Chem. Commun.* **2008**, *11*, 643. (b) Papish, E. T.; Taylor, M. T.; Jernigan, F. E., III; Rodig, M. J.; Shawhan, R. R.; Yap, G. P. A.; Jove, F. A. *Inorg. Chem.* **2006**, *45*, 2242.

(12) Ferreira, K. N.; Iverson, T. M.; Maghlaoui, K.; Barber, J.; Iwata, S. *Science* **2004**, *303*, 1831.

(13) (a) Chakraborty, J.; Thakurta, S.; Pilet, G.; Luneau, D.; Mitra, S. *Polyhedron* **2009**, *28*, 819−825. (b) Burkhardt, A.; Spielberg, E. T.; Gorls, H.; Plass, W. *Inorg. Chem.* **2008**, *47*, 2485−2493. (c) Mukherjee, A.; Raghunathan, R.; Saha, M. K.; Nethaji, M.; Ramasesha, S.; Chakravarty, A. R. *Chem.—Eur. J.* **2005**, *11*, 3087−3096.

(14) (a) Erxleben, A. *Inorg. Chem.* **2001**, *40*, 208−213. (b) Tong, M. L.; Zheng, S. L.; Shi, J. X.; Tong, Y. X.; Lee, H. K.; Chen, X. M. *J. Chem. Soc., Dalton Trans.* **2002**, 1727−1734. (c) Papatriantafyllopoulou, C.; Efthymiou, C. G.; Raptopoulou, C. P.; Vicente, R.; Manessi-Zoupa, E.; Psycharis, V.; Escuer, A.; Perlepes, S. P. *J. Mol. Struct.* **2007**, *829*, 176−188.

(15) (a) Zhang, S. H.; Li, N.; Ge, C. M.; Feng, C.; Ma, L. F. *Dalton Trans.* **2011**, *40*, 3000−3007. (b) Hazra, S.; Koner, R.; Lemoine, P.; Sanudo, E. C.; Mohanta, S. *Eur. J. Inorg. Chem.* **2009**, 3458−3466. (c) Efthymiou, C. G.; Raptopoulou, C. P.; Terzis, A.; Boca, R.; Korabic, M.; Mrozinski, J.; Perlepes, S. P.; Bakalbassis, E. G. *Eur. J. Inorg. Chem.* **2006**, 2236−2252. (d) Escuer, A.; Font-Bardia, M.; Kumar, S. B.; Solans, X.; Vicente, R. *Polyhedron* **1999**, *18*, 909−914.

(16) (a) Dismukes, G. C.; Brimblecombe, R.; Felton, G. A. N.; Pryadun, R. S.; Sheats, J. E.; Spiccia, L.; Swiegers, G. F. *Acc. Chem. Res.* **2009**, *42*, 1935−1943. (b) Ruettinger, W. F.; Ho, D. M.; Dismukes, G. C. *Inorg. Chem.* **1999**, *38*, 1036−1037. (c) Aromi, G.; Bhaduri, S.; Artus, P.; Folting, K.; Christou, G. *Inorg. Chem.* **2002**, *41*, 805−817. (d) Papaefstathiou, G. S.; Escuer, A.; Mautner, F. A.; Raptopoulou, C.; Terzis, A.; Perlepes, S. P.; Vicente, R. *Eur. J. Inorg. Chem.* **2005**, 879−893. (e) Stoumpos, C. C.; Gass, I. A.; Milios, C. J.; Lalioti, N.; Terzis, A.; Aromi, G.; Teat, S. J.; Brechin, E. K.; Perlepes, S. P. *Dalton Trans.* **2009**, 307−317. (f) Shiga, T.; Oshio, H. *Sci. Technol. Adv. Mater.* **2005**, *6*, 565−570.

(17) (a) Shoner, S. C.; Power, P. P. *Inorg. Chem.* **1992**, *31*, 1001−1010. (b) Oshio, H.; Hoshino, N.; Ito, T.; Nakano, M. *J. Am. Chem. Soc.* **2004**, *126*, 8805−8812.

(18) (a) Isele, K.; Gigon, F.; Williams, A. F.; Bernardinelli, G.; Franz, P.; Decurtins, S. *Dalton Trans.* **2007**, 332−341. (b) Ama, T.; Rashid, M. M.; Yonemura, T.; Kawaguchi, H.; Yasui, T. *Coord. Chem. Rev.* **2000**, *198*, 101−116. (c) McCool, N. S.; Robinson, D. M.; Sheats, J. E.; Dismukes, G. C. *J. Am. Chem. Soc.* **2011**, *133*, 11446−11449.

(19) Hendrickson, D. N.; Christou, G.; Schmitt, E. A.; Libby, E.; Bashkin, J. S.; Wang, S.; Tsai, H. L.; Vincent, J. B.; Boyd, P. D. W. *J. Am. Chem. Soc.* **1992**, *114*, 2455.

(20) Kampert, E.; Janssen, F. F. B. J.; Boukhvalov, D. W.; Russcher, J. C.; Smits, J. M. M.; de Gelder, R.; de Bruin, B.; Christianen, P. C. M.; Zeitler, U.; Katsnelson, M. I.; Maan, J. C.; Rowan, A. E. *Inorg. Chem.* **2009**, *48*, 11903.

(21) (a) McCall, K. A.; Huang, C. C.; Fierke, C. A. *J. Nutr.* **2000**, *130*, 1437S−1446S. (b) Maret, W. *J. Inorg. Biochem.* **2012**, *111*, 110−116.

(22) Lane, T. W.; Saito, M. A.; George, G. N.; Pickering, I. J.; Prince, R. C.; Morel, F. M. M. *Nature* **2005**, *435*, 42−42.

(23) (a) Xu, Y.; Feng, L.; Jeffrey, P. D.; Shi, Y. G.; Morel, F. M. M. *Nature* **2008**, *452*, 56−61. (b) Amata, O.; Marino, T.; Russo, N.; Toscano, M. *Phys. Chem. Chem. Phys.* **2011**, *13*, 3468−3477.

(24) Liles, D. C.; Mcpartlin, M.; Tasker, P. A.; Lip, H. C.; Lindloy, L. F. J. *Chem. Soc., Chem. Commun.* **1976**, *14*, 549.

(25) (a) Vincent, J. B.; Christmas, C.; Chang, H. R.; Li, Q.; Boyd, P. D. W.; Huffman, J. C.; Hendrickson, D. N.; Christou, G. *J. Am. Chem. Soc.* **1989**, *111*, 2086−2097. (b) Bagai, R.; Christou, G. *Chem. Soc. Rev.* **2009**, *38*, 1011−1026. (c) Chakov, N. E.; Lee, S. C.; Harter, A. G.; Kuhns, P. L.; Reyes, A. P.; Hill, S. O.; Dalal, N. S.; Wernsdorfer, W.; Abboud, K. A.; Christou, G. *J. Am. Chem. Soc.* **2006**, *128*, 6975−6989.

(26) (a) Sessoli, R.; Tsai, H. L.; Schake, A. R.; Wang, S. Y.; Vincent, J. B.; Folting, K.; Gatteschi, D.; Christou, G.; Hendrickson, D. N. *J. Am. Chem. Soc.* **1993**, *115*, 1804−1816. (b) Liu, S.; Bremer, M. T.; Lovaasen, J.; Caruso, A. N.; O'Neill, K.; Simpson, L.; Parilla, P. A.; Heben, M. J.; Schulz, D. L. *Inorg. Chem.* **2008**, *47*, 1568−1575.

(27) Demsar, A.; Kosmrlj, J.; Petricek, S. *J. Am. Chem. Soc.* **2002**, *124*, 3951.

(28) Caudle, M. T.; Brennessel, W. W.; Young, V. G., Jr. *Inorg. Chem.* **2005**, *44*, 3233.

(29) (a) Feng, M.; Gu, C.; Mi, H. F.; Hu, T. L. *Acta Crystallogr., Sect. E* **2011**, *67*, m520. (b) Carballo, R.; Covelo, B.; Vazquez-Lopez, E. M.; Garcia-Martinez, E.; Castineiras, A. *Z. Anorg. Allg. Chem.* **2002**, *628*, 907−908.

(30) (a) Soler, M.; Artus, P.; Folting, K.; Huffman, J. C.; Hendrickson, D. N.; Christou, G. *Inorg. Chem.* **2001**, *40*, 4902−4912. (b) Chisholm, M. H.; Macintosh, A. M. *J. Chem. Soc., Dalton Trans.* **1999**, 1205−1207.

(31) The ratio between acetate and benzoate, determined from the crystal structure, is not an exact number, and could well be a superposition of the statistical mixture in the solid state.